Spin-Orbit Coupling in the Mott Insulator Ca_2RuO_4

T. Mizokawa,[1,2] L. H. Tjeng,[2] G. A. Sawatzky,[2] G. Ghiringhelli,[3,4] O. Tjernberg,[3,5] N. B. Brookes,[3] H. Fukazawa,[6] S. Nakatsuji,[6] and Y. Maeno[6,7]

[1]*Department of Complexity Science and Engineering, University of Tokyo, Tokyo 113-0033, Japan*
[2]*Materials Science Centre, University of Groningen, 9747 AG Groningen, The Netherlands*
[3]*European Synchrotron Radiation Facility, BP 220, 38043, Grenoble, France*
[4]*INFM, Dipartimento di Fisica, Politecnico di Milano, piazza Leonardo da Vinci 32, 20133 Milano, Italy*
[5]*Materials Physics, KTH, S-100 44 Stockholm, Sweden*
[6]*Kyoto University, Kyoto 606-8502, Japan*
[7]*CREST, Japan Science and Technology Corporation, Kawaguchi, Saitama 332-0012, Japan*
(Received 10 October 2000; published 30 July 2001)

O 1*s* x-ray absorption study of the Mott insulator Ca_2RuO_4 shows that the orbital population of the 4*d* t_{2g} band dramatically changes with temperature. In addition, spin-resolved circularly polarized photoemission study of Ca_2RuO_4 shows that a substantial orbital angular momentum is induced in the Ru 4*d* t_{2g} band. Based on the experimental results and model Hartree-Fock calculations, we argue that the cooperation between the strong spin-orbit coupling in the Ru 4*d* t_{2g} band and the small distortion of the RuO_6 octahedra causes the interesting changeover of the spin and orbital anisotropy as a function of temperature.

DOI: 10.1103/PhysRevLett.87.077202 PACS numbers: 75.25.+z, 78.70.Dm, 79.60.Bm

The layered perovskites Sr_2RuO_4 and Ca_2RuO_4 show interesting and contrasting physical properties. While Sr_2RuO_4 is metallic and shows superconductivity below 1.5 K [1], Ca_2RuO_4 is insulating and becomes antiferromagnetic below 110 K [2,3]. In Sr_2RuO_4 and Ca_2RuO_4, four electrons occupy the three nearly degenerate 4*d* t_{2g} orbitals and the orbitals degree of freedom are expected to be important. Since the spin-orbit interaction in the 4*d* shell is substantial, the orbital angular momentum *L* can strongly couple with the spin angular momentum *S*. Triplet pairing in the superconducting Sr_2RuO_4 has been predicted by Rice and co-workers [4] and is supported by recent experimental studies [5]. However, it is still controversial how strongly the 4*d* electrons are correlated in this metal and it is not well understood how the spin and orbital fluctuations are related to the triplet superconductivity [6,7]. Ca_2RuO_4, on the other hand, is widely accepted as a Mott insulator since it remains insulating above the Néel temperature and shows a Curie-Wiess magnetic susceptibility [2]. With the 4*d* electrons being localized, Ca_2RuO_4 gives us an opportunity to study the interplay between the spin and orbital degrees of freedom, which could provide a clue to understanding their roles in the triplet superconductivity of the layered Ru oxides.

We have measured the Ru 4*d* orbital population using O 1*s* x-ray absorption spectroscopy (XAS), and have discovered that the orbital population changes dramatically between 90 and 300 K. This is remarkable in view of the modest temperature dependence of the crystal structure [3]: at 300 K the RuO_6 octahedron is almost regular and at 90 K it becomes slightly flattened along the *c* axis by not more than about 2.5%. Using spin-resolved circularly polarized photoemission, we conclude that the Ru 4*d* band has a substantial orbital angular momentum, and in combination with model Hartree-Fock calculations, we infer that the strong spin-orbit interaction cooperates with the small distortion of the RuO_6 octahedra to cause a major change in the spin and orbital anisotropy as a function of temperature.

The experiments were performed using the helical undulator [8] based beam line ID12B [9] at the European Synchrotron Radiation Facility at Grenoble. Circularly polarized light was used for both the XAS and photoemission, and the degree of circular polarization was ≈92%. The XAS data were taken in the total electron yield mode as a function of the angle θ between the surface normal and the Poynting vector of the circularly polarized light. The photon energy resolution is better than 0.15 eV. The photoemission spectra were recorded at normal emission with $\theta = 60°$ using a 140 mm mean radius hemispherical analyzer coupled to a mini-Mott 25 kV spin polarimeter [10]. The total energy resolution was about 1 eV, and the spin detector had an efficiency (Sherman function) of 17%. The photoemission spectra were taken in the four possible combinations of photon helicity (σ^+/σ^-) and electron spin direction ($e^{\uparrow}/e^{\downarrow}$ measured simultaneously) in order to eliminate systematic errors. The pressure of the spectrometer chamber was 1×10^{-10} mbar. The single crystals of Ca_2RuO_4, grown by a floating zone method as reported in the literature [11], were cleaved *in situ*. The cleaved surface is parallel to the *ab* plane or the RuO_2 plane.

Figure 1 shows the O 1*s* XAS spectra taken at 90 and 300 K at the normal light incidence ($\theta = 0°$). The structures from 528 to 530 eV and those from 530 to 535 eV are due to transitions from the O 1*s* core level to the O 2*p* orbitals that are mixed into the unoccupied Ru 4*d* t_{2g} and e_g

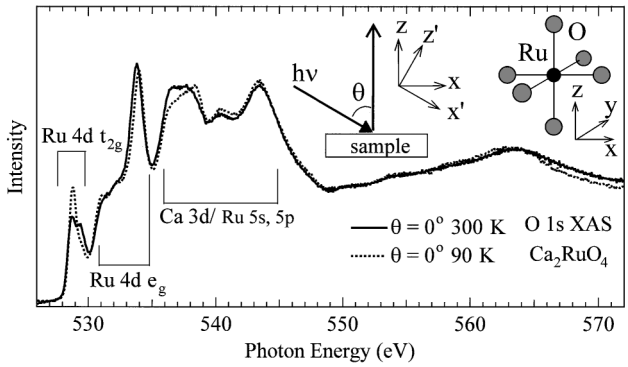

FIG. 1. O 1s x-ray absorption spectra of Ca_2RuO_4 taken at 90 and 300 K at normal incidence. The spectra are normalized using the higher energy region above 550 eV. The insets show schematic pictures of the experimental arrangement and the RuO_6 octahedron.

states, respectively. The structures from 535 to 550 eV are derived from transitions to the O $2p$ orbitals mixed into the Ca $3d$/Ru $5s, 5p$ states. The XAS spectra are normalized using the higher energy region above 550 eV. In going from 300 to 90 K, the e_g-derived structures become somewhat sharper and the Ca $3d$ feature changes its line shape. This is because the tilting of the RuO_6 octahedra increases with cooling [3] and, consequently, e_g band width is reduced and the Ca-O bond length is changed. The t_{2g} features, on the other hand, show dramatic changes with temperature, and this requires an explanation in terms of changes of the t_{2g} orbital occupations, which is the main object of the following discussions.

Figure 2 shows the Ru $4d$-derived O 1s XAS spectra taken at 90 and 300 K for θ varying between 0° and 70°. In the e_g-derived region above 530 eV, the structures at ~531 and 534 eV increase and decrease with θ, respectively, indicating that the lower and higher energy regions of the e_g band are mainly constructed from the $2p_\sigma$ states at the apical and in-plane oxygen sites, respectively. This is consistent with the recent band-structure calculation for Ca_2RuO_4 [12]. In the t_{2g}-derived region, the two peaks located at 528.5 and 529.5 eV (labeled as A and B, respectively) show a very distinct angular dependence. Since the apical oxygen XAS peak is lower in energy than the in-plane one for $La_{2-x}Sr_xCuO_4$ [13] and Sr_2RuO_4 [14], we can assign structures A and B to transitions at the apical and in-plane oxygen sites, respectively. This assignment is also supported by the observation that the intensity of structure A relative to that of B is much smaller in Sr_2RuO_4 [14] than in Ca_2RuO_4, consistent with the fact that the RuO_6 octahedra are appreciably elongated in Sr_2RuO_4 along the c axis while they are almost regular in Ca_2RuO_4. We will now use the angular dependence of the apical and in-plane features to determine the t_{2g} orbital population.

In order to extract estimates from the spectra, we fit them with a Gaussian for each of structures A and B and with a Gaussian to represent the tail of the higher lying e_g band.

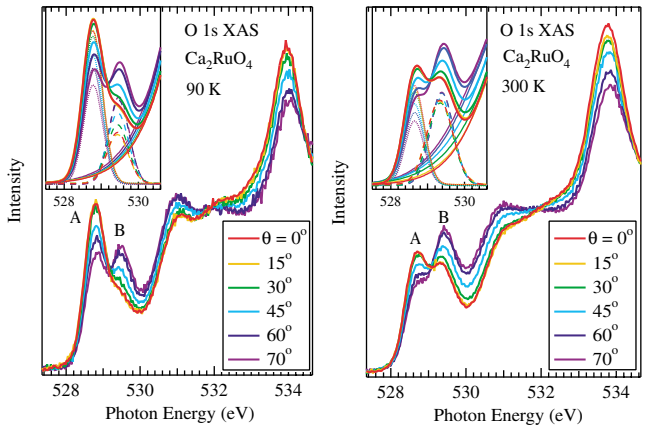

FIG. 2 (color). O 1s x-ray absorption spectra of Ca_2RuO_4 taken at 90 and at 300 K as a function of angle θ, which is the angle between the surface normal and the Poynting vector of the circularly polarized light. The spectra are normalized using the higher energy region above 550 eV. In the insets, the fitted results are shown by the thick solid curves. The two Gaussians for structures A and B, and the tail of another Gaussian for the e_g band are shown by the dotted, dashed, and solid curves, respectively.

The fits are shown by the thick solid curves in the insets of Fig. 2 and the extracted intensities of the apical and in-plane components are depicted in Figs. 3(a) and 3(b) as a function of θ. The angular dependence is determined by the dipole matrix element of the O 1s-2p transition. For circularly polarized light, transitions to the O $2p_x$, $2p_y$, and $2p_z$ orbitals have θ dependences of $\frac{1}{2}\cos^2\theta$, $\frac{1}{2}$, and $\frac{1}{2}\sin^2\theta$, respectively. Since the $2p_x/2p_y$ and $2p_z$ orbitals of the in-plane oxygen hybridize with the xy and yz/zx states, respectively, the in-plane component has the θ dependence of $\frac{1}{2}(\cos^2\theta + 1)n_{xy} + \frac{1}{2}\sin^2\theta n_{yz/zx}$. Here, n_{xy} and $n_{yz/zx}$ are the number of *holes* in the xy and yz/zx states, respectively. On the other hand, since the $2p_x(2p_y)$ orbital of the apical oxygen hybridizes with the $zx(yz)$ state, the apical component is given by $\frac{1}{2}(\cos^2\theta + 1) \times n_{yz/zx}$. With Ca_2RuO_4 having two holes in the $4d$ t_{2g} orbitals ($n_{xy} + n_{yz/zx} = 2$), we can simulate the θ dependence for a certain n_{xy}:$n_{yz/zx}$ ratio. Taking into account the small effect of the tilting of the octahedra, we have plotted the results for n_{xy}:$n_{yz/zx} = \frac{1}{2}$:$\frac{3}{2}$ and n_{xy}:$n_{yz/zx}$ = 1:1 in Figs. 3(c) and 3(d), respectively. The experimental results at 90 K agree well with the simulation in Fig. 3(c), and those at 300 K with the simulation in Fig. 3(d). In addition, since we have incorporated the bond-length dependence of the Ru-O hybridization strength in the simulations [15], we are also able to reproduce the ratio between the apical and in-plane components. These angle dependent results thus indicate that the relative hole population between the xy and yz/zx orbitals is roughly 1:1 at 300 K and is drastically changed to roughly $\frac{1}{2}$:$\frac{3}{2}$ at 90 K. Here, it should be noted that these numbers are obtained using the simple hybridization model which can provide only

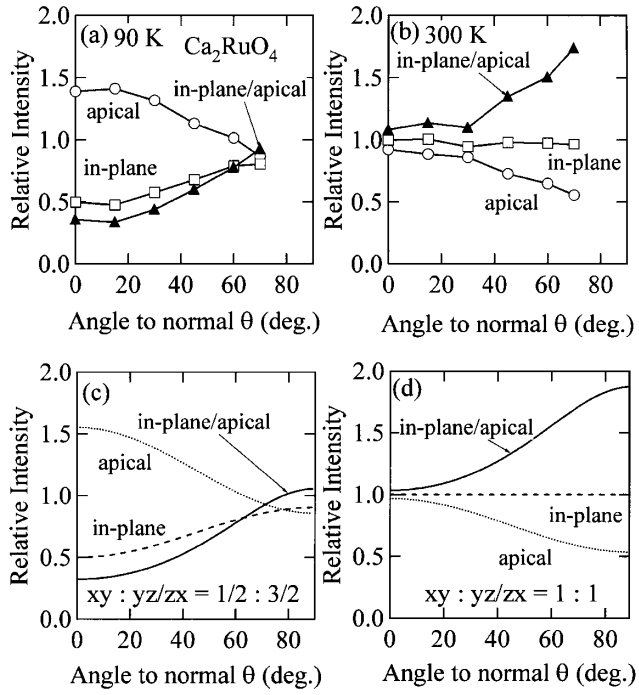

FIG. 3. Upper two panels: Intensities of the apical component (open circles) and in-plane component (open squares) and the ratio between the two components (closed triangles) as a function of angle θ in the O 1s x-ray absorption spectra taken at 90 K (a) and 300 K (b). Lower two panels: Intensities of the apical component (dotted curve), in-plane component (dashed curve), and the ratio between the two components (solid curves) as a function of θ obtained by model calculation for the orbital population of n_{xy}:$n_{yz/zx} = \frac{1}{2}:\frac{3}{2}$ (c) and of n_{xy}:$n_{yz/zx} = 1{:}1$ (d).

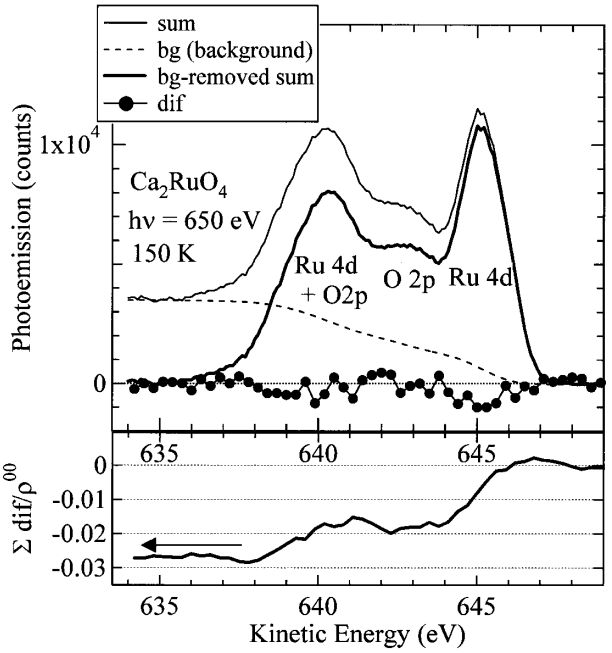

FIG. 4. Valence-band photoemission spectra of Ca_2RuO_4. The thin solid curve and closed circles show the sum and difference of the spectra taken with parallel and antiparallel alignment. The dashed curve and thick solid curve indicate the background due to secondary electrons and the background-removed sum spectrum, respectively. In the lower panel, the difference spectrum normalized to ρ^{00} is integrated from the higher kinetic energy side.

a rough estimation of the orbital population. In order to quantitatively understand the orbital state in Ca_2RuO_4, the hybridization between the Ru 4d and O 2p orbitals should be taken into account in a more accurate way.

In order to elucidate the possible role of the Ru 4d spin-orbit interaction and its consequences for the spin and orbital states, we have also measured the spin-resolved valence band photoemission spectrum of Ca_2RuO_4 using circularly polarized light. It has been shown recently that this type of spectroscopy is very useful to investigating the spin and orbital contributions to the magnetic moments in especially antiferromagnets and paramagnets [16]. Figure 4 shows the photoemission spectrum taken at 150 K (above the Néel temperature) with a photon energy ($h\nu$) of 650 eV. The thin solid curve and closed circles depict the sum and the difference, respectively, of the spectra taken with parallel ($\sigma^+e^\uparrow$ and $\sigma^-e^\downarrow$) and antiparallel ($\sigma^+e^\downarrow$ and $\sigma^-e^\uparrow$) alignment of the photon helicity and electron spin. The structures at the kinetic energies of 645, 643, and 640 eV in the sum spectrum are derived from the Ru 4d band, the O 2p band, and the O 2p-Ru 4d hybridized band, respectively [12]. In the difference spectrum, the spectral weight is mainly on the Ru 4d band and the O 2p-Ru 4d hybridized band indicating that the spin polarization induced by the spin-orbit coupling is dominated by the Ru 4d contribution. The quantity of interest here is the ratio between the integrated intensity of the difference spectrum (ρ^{11}) and that of the isotropic spectrum (ρ^{00}), which is equal to $\frac{3}{2}$ times the sum spectrum [17]. This ratio can be related to the expectation value of a spin-orbit operator of the system in the initial state, which for transitions from 4d to ϵf like final states is given by [17]:

$$\frac{\rho^{11}}{\rho^{00}} = \frac{2\langle\sum_i l_{x'}(i)\cdot s_x(i)\rangle}{3N_d}, \qquad (1)$$

where N_d denotes the number of 4d electrons, i is an index of the electrons, and $l_{x'}$ and s_x are the orbital and spin angular momentum along the x and x' direction of the ith electron, respectively (see the inset of Fig. 1). We find that the ratio converges to -0.027 ± 0.007, as shown in the lower panel of Fig. 4. In order to estimate the polarization of the Ru t_{2g} band, one needs to subtract the contribution of the O 2p band from ρ^{00}. Since the photoionization cross section of the O 2p relative to that of the Ru 4d is $\sim$0.7 [18], the polarization of the Ru 4d band is estimated to be -0.046 ± 0.012. This means that $\langle\sum_i l_{x'}(i)\cdot s_x(i)\rangle$ is about -0.28 ± 0.07, using $N_d = 4$. This value is comparable to that measured for CoO [16], where the orbital moment was found to be of the order of 1 μ_B. These measurements thus demonstrate that the

strong Ru $4d$ spin-orbit interaction induces a substantial orbital angular momentum in Ca_2RuO_4.

Combining the orbital population obtained from the O $1s$ XAS data with the substantial orbital angular momentum L, it is natural to speculate that the two holes are sitting at the yz and $(xy + izx)/\sqrt{2}$ orbitals [or zx and $(yz + ixy)/\sqrt{2}$ orbitals] at 90 K. With this spin and orbital state, S and L are expected to be along the x axis (or the y axis). On the other hand, at 300 K, the two holes are sitting at the xy and $(zx + iyz)/\sqrt{2}$ orbitals at each Ru site, and, consequently, S and L tend to be directed towards the z axis, although they are not perfectly aligned above the Néel temperature. In this scenario, the cooperation between the strong spin-orbit coupling and the small compression of the RuO_6 octahedra as discussed in [19] induces the drastic change of the orbital population observed in the O $1s$ XAS measurement.

In order to check possible spin and orbital states in Ca_2RuO_4, we have performed Hartree-Fock calculations using a multiband Ru $4d$-O $2p$ model for a Ru-O slab constructed from the RuO_6 octahedra. The intra-atomic Coulomb interaction between the $4d$ electrons is included using Kanamori parameters u, u', j, and j' ($u' = u - 2j$, $j = j'$, $j = \frac{5}{2}B + C$, where B and C are Racah parameters) [20]. j (= 0.5 eV) and the spin-orbit coupling ξ_d (= 0.15 eV) are fixed to the atomic values. The O $2p$-to-Ru $4d$ charge-transfer energy Δ (= 0.0 eV), the multiplet-averaged d-d Coulomb interaction U ($\equiv u - \frac{20}{9}j$ = 3.0 eV), and the Ru $4d$-O $2p$ and O $2p$-O $2p$ transfer integrals are deduced from the LDA calculations for Ca_2RuO_4 [12] and photoemission and optical study of (Ca, Sr)RuO_3 [21]. When the lattice is distorted, the transfer integrals are scaled using Harrison's prescription [15]. Although the uncertainty of Δ and U is ± 1 eV, it does not affect the conclusion. When the RuO_6 octahedra are regular or elongated, the antiferromagnetic state with the two holes in the xy and $(zx + iyz)/\sqrt{2}$ orbitals is stable and S (0.80) and L (0.72) are directed towards the z axis. On the other hand, when the RuO_6 octahedra are slightly compressed (the in-plane Ru-O bond is by 2.5% longer than the apical one), the yz/zx orbitals become higher in energy compared to the xy orbitals. Consequently, the antiferromagnetic state with the two holes in the yz and $(xy + izx)/\sqrt{2}$ orbitals [zx and $(yz + ixy)/\sqrt{2}$ orbitals] is stabilized and S (0.80) and L (0.68) are directed towards the x axis (y axis). The energy of the latter solution relative to the former one is 30, 15, and -82 meV for the elongated, regular, and compressed cases, respectively. L is $\sim$0.7 for the three cases because the splitting between the xy and yz/zx orbitals is smaller than the strong spin-orbit coupling. The total angular momentum $L + 2S$ is calculated to be $\sim$2.3 μ_B which is reduced from the atomic value because of the strong covalency between the Ru $4d$ and O $2p$ orbitals and is consistent with the effective Bohr magneton number obtained from the magnetic susceptibility [19]. Spin fluctuations due to the two dimensionality and the remaining orbital fluctuations might be responsible for the reduction of the ordered moment ($1.3\mu_B$) [3].

In conclusion, the spin-resolved circularly polarized photoemission measurement of Ca_2RuO_4 has revealed that the strong spin-orbit coupling induces the substantial orbital angular momentum in the Ru $4d$ t_{2g} band. The large temperature dependence of the O $1s$ XAS data shows that the orbital population of the t_{2g} band is drastically changed by the small compression of the RuO_6 octahedra and the strong spin-orbit interaction. In the future, the present technique should be applied to $Ca_{2-x}Sr_xRuO_4$ in order to further elucidate the spin and orbital fluctuations and their relations with the triplet superconductivity.

The authors would like to thank K. Larsson for his skillful technical support and A. Tanaka and T. Jo for valuable comments. This work was supported by the Nederlands Organization for Fundamental Research of Matter with financial support from the Netherlands Organization for the Advancement of Pure Research and by the European Commission TRM network on Oxide Spin Electronics.

[1] Y. Maeno *et al.,* Nature (London) **372**, 532 (1994); A. P. Mackenzie *et al.,* Phys. Rev. Lett. **80**, 161 (1998).
[2] S. Nakatsuji, S. Ikeda, and Y. Maeno, J. Phys. Soc. Jpn. **66**, 1868 (1997).
[3] M. Braden *et al.,* Phys. Rev. B **58**, 847 (1998); O. Friedt *et al.,* cond-mat/0007218.
[4] T. M. Rice and M. Sigrist, J. Phys. Condens. Matter **7**, L643 (1995).
[5] G. M. Luke *et al.,* Nature (London) **394**, 558 (1998); K. Ishida *et al.,* Nature (London) **396**, 658 (1998).
[6] D. F. Agterberg, T. M. Rice, and M. Sigrist, Phys. Rev. Lett. **78**, 3374 (1997).
[7] I. I. Mazin and D. J. Singh, Phys. Rev. Lett. **79**, 733 (1997); **82**, 4324 (1999).
[8] P. Elleaume, J. Synchrotron Radiat. **1**, 19 (1994).
[9] J. Goulon *et al.,* Physica (Amsterdam) **208B**, 199 (1995).
[10] G. Ghiringhelli *et al.,* Rev. Sci. Instrum. **70**, 4225 (1999).
[11] H. Fukazawa, S. Nakatsuji, and Y. Maeno, Physica (Amsterdam) **281B–282B**, 613 (2000).
[12] L. M. Woods, Phys. Rev. B **62**, 7833 (2000).
[13] C. T. Chen *et al.,* Phys. Rev. Lett. **66**, 104 (1991).
[14] M. Schmidt *et al.,* Phys. Rev. B **53**, R14 761 (1996).
[15] W. A. Harrison, *Electronic Structure and the Properties of Solids* (Dover, New York, 1989).
[16] G. Ghiringhelli *et al.* (to be published).
[17] G. van der Laan and B. T. Thole, Phys. Rev. B **48**, 210 (1993).
[18] J. J. Yeh and I. Lindau, At. Data Nucl. Data Tables **32**, 1 (1985).
[19] S. Nakatsuji and Y. Maeno, Phys. Rev. Lett. **84**, 2666 (2000); Phys. Rev. B **62**, 6458 (2000).
[20] J. Kanamori, Prog. Theor. Phys. **30**, 275 (1963).
[21] K. Fujioka *et al.,* Phys. Rev. B **56**, 6380 (1997); J. S. Ahn *et al.,* Phys. Rev. Lett. **82**, 5321 (1999).